パーキンソン病の病態と成因

パーキンソン病（PD）は65歳以上の高齢者の5％に発症する神経変性疾患であり，臨床医が遭遇する変性疾患としてはアルツハイマー病に次いで頻度の高いものである。近年20年間の神経科学の進歩により多くの単遺伝子に由来するPDの病因遺伝子が見出された(表1)[1]。しかし，PDのなかで90％以上を占める孤発性の疾患の原因はいまだに不明であり，老化に伴う神経細胞の機能異常が重要な役割を果たしていると考えられる。遺伝子変異を持つ家族性PDの症例においてもある一定度以上の加齢（老化）が起こらなければ疾病の発症に至らないこともこれを示唆している。

では，老化の本体は何なのであろうか。老化は加齢に伴って起こる心身の機能低下と考えられるが，その本体は不明である。しかし，老化の学説のなかでも1956年にD. Harmanによって提唱されたフリーラジカル説は多くの老化研究者の賛同を得ている。フリーラジカルによる生体分子（蛋白質，核酸，脂質など）の障害の蓄積が長期間の後に生体機能の障害の原因となると考えられる。

分裂細胞，分裂終了細胞の両者共に老化が起こるが，分裂能の極めて低い神経細胞の老化は個体老化においてより重要な役割を果たしていると考えられている。さらに，脳神経細胞は不飽和脂肪酸を多量に含むこと，好気的呼吸に依存性が高いことなどのため，酸化ストレスが常に高いレベルに保たれている。現在，PDにおける異常蛋白質，特にα-シヌクレインの蓄積は神経細胞死の原因として注目されている。剖検脳の分析や，病因遺伝子の解析結果から，孤発性パーキンソン病ではミトコンドリア機能不全・酸化ストレス・蛋白質分解系の機能不全の悪性サイクル（vicious cycle）が起動されることにより，最終的に異常蛋白質の蓄積と，細胞死が引き起こ

表1　家族性PDの原因遺伝子

	Locus	Gene	Function
Park 1	4q21-22	α-synuclein	presynaptic
Park 2	6q25-27	Parkin	E3 ubiquitin ligase
Park 5	4p14	UCH-L1	ubiquitin recycling enzyme
Park 6	1p25-36	PINK1	mitochondrial
Park 7	1p36	DJ1	oxidative stress response
Park 8	12p11.2q13.1	LRRK2	kinase

（文献1より引用）

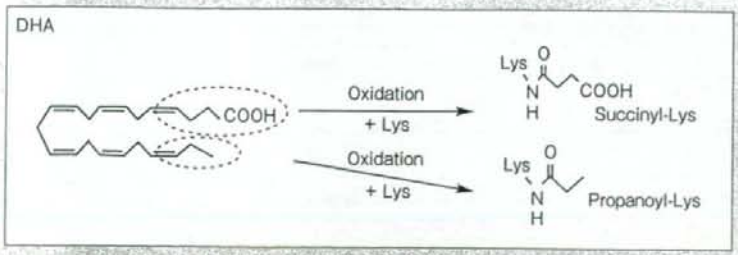

図1　膜脂質を構成する多価不飽和脂肪酸の酸化と蛋白質修飾

されるとの考えが主流となっている。

PDのドパミン神経細胞において蓄積するα-シヌクレインはシナプス膜，特に不飽和脂肪酸と緩やかに結合して構造を安定化させていることが知られている。生体膜は，細胞の外側を構成しているだけでなくミトコンドリアなどの細胞内小器官の構成物としても重要な役割を持っている。特に，神経細胞膜の脂質のなかにはリン脂質として不飽和脂肪酸エステルが多く含まれており，シナプスの可塑性や膜に存在する蛋白質の流動性に重要な役割を果たしていると考えられている。特に，脳内に多量に含まれる魚油由来のn-3系多価不飽和脂肪酸であるdocosahexaenoic acid（DHA）摂取とPD，アルツハイマー病については多くの疫学研究で，予防効果が報告されている。しかし，不飽和脂肪酸は酸化傷害を容易に受ける分子でもあり，老化に伴い酸化が進行することが報告されている。図1にDHAの酸化による開裂とアミノ酸であるリジンとの結合について示した．α-シヌクレインはこのような脂質過酸化物のターゲットとなるアミノ酸分子を複数含有するため，細胞膜との結合係数の変化，あるいは蛋白質自身の構造変化によってPD発症のtriggerとなる可能性がある。

その他，老化に伴い異常蛋白質分解の要であるproteasome活性の低下，あるいはミトコンドリア機能の低下などが報告されており，家族性PDと類似した病態が孤発性PDでも複合的に引き起こされている可能性がある。

以上，今後のPD研究においては，加齢（正常）と老化（異常），健康と疾病を分かつものが何かを見極めていくことが重要であろう。

REFERENCES

1）Fleming SM, Fernagut PO, Chesselet MF: Genetic mouse models of parkinsonism: strengths and limitations. NeuroRx 2: 495-503, 2005

AMERICAN JOURNAL OF PHYSICAL ANTHROPOLOGY 135:182–194 (2008)

Development of the Supralaryngeal Vocal Tract in Japanese Macaques: Implications for the Evolution of the Descent of the Larynx

Takeshi Nishimura,[1]* Takao Oishi,[2] Juri Suzuki,[3] Keiji Matsuda,[4] and Toshimitsu Takahashi[5]

[1]*Laboratory of Physical Anthropology, Department of Zoology, Graduate School of Science, Kyoto University, Sakyo, Kyoto 606-8502, Japan*
[2]*Department of Cellular and Molecular Biology, Primate Research Institute, Kyoto University, Inuyama, Aichi 484-8506, Japan*
[3]*Center for Human Evolution Modeling Research, Primate Research Institute, Kyoto University, Inuyama, Aichi 484-8506, Japan*
[4]*Systems Neuroscience Group, Neuroscience Research Institute, National Institute of Advanced Industrial Science and Technology, Tsukuba, Ibaragi 305-8568, Japan*
[5]*Department of Neurophysiology, Juntendo University, Graduate School of Medicine, Bunkyo, Tokyo 113-8421, Japan*

KEY WORDS descent of the hyoid; hyo-laryngeal complex; epiglottis; *Macaca fuscata*; MRI

ABSTRACT The configuration of the supralaryngeal vocal tract depends on the nonuniform growth of the oral and pharyngeal portion. The human pharynx develops to form a unique configuration, with the epiglottis losing contact with the velum. This configuration develops from the great descent of the larynx relative to the palate, which is accomplished through both the descent of the laryngeal skeleton relative to the hyoid and the descent of the hyoid relative to the palate. Chimpanzees show both processes of laryngeal descent, as in humans, but the evolutionary path before the divergence of the human and chimpanzee lineages is unclear. The development of laryngeal descent in six living Japanese macaque monkeys, *Macaca fuscata*, was examined monthly during the first three years of life using magnetic resonance imaging, to delineate the present or absence of these two processes and their contributions to the development of the pharyngeal topology. The macaque shows descent of the hyoid relative to the palate, but lacks the descent of the laryngeal skeleton relative to the hyoid and that of the EG from the VL. We argue that the former descent is simply a morphological consequence of mandibular growth and that the latter pair of descents arose in a common ancestor of extant hominoids. Thus, the evolutionary path of the great descent of the larynx is likely to be explained by a model comprising multiple and mosaic evolutionary pathways, wherein these developmental phenomena may have contributed secondarily to the faculty of speech in the human lineage. Am J Phys Anthropol 135:182–194, 2008.

Adult humans have a unique anatomy of the supralaryngeal vocal tract (SVT), with equally long horizontal oral and vertical pharyngeal cavities, in contrast to all nonhuman primates having a pharynx much shorter than the oral cavity (Negus, 1949; Lieberman, 1984). Such a configuration of human SVT depends on the nonuniform growth of the oral and pharyngeal portions with a faster growth rate in the latter than the former (Negus, 1949; Lieberman, 1984; Crelin, 1987). Adult humans have a unique anatomy of the pharynx, with the epiglottis losing contact with the velum during development. This configuration secures a long oropharyngeal region facing the dorsal surface of the mobile tongue, rostral to the laryngopharyngeal region that faces the epiglottis (Lieberman, 1984; Crelin, 1987; Zemlin, 1988). This anatomy of the human pharynx is formed ontogenetically with the great descent of the larynx relative to the palate (Negus, 1949; Roche and Barkla, 1965; Lieberman, 1984; Crelin, 1987; Westhorpe, 1987; Zemlin, 1988). The laryngeal skeleton is suspended from the hyoid apparatus and the hyoid is in turn suspended from the mandible and cranial base by muscles and ligaments (Zemlin, 1988; Williams, 1995). Anatomically, two processes accomplish the great descent of the larynx in humans: the descent of the laryngeal skeleton relative to the hyoid, and the descent of the hyoid relative to the palate. One or both of them cause the epiglottis—attached to the thyroid cartilage of the laryngeal skeleton—to descend along the neck and to lose contact with the velum.

All nonhuman primates have a pharynx much shorter than the oral cavity (Negus, 1949; Laitman and Reidenberg, 1993), although they show the descent of the larynx relative to the palate that lengthens the pharyngeal cavity during growth (Flügel and Rohen, 1991). Such a SVT configuration makes the great descent of the larynx

Grant sponsor: Japan Society for the Promotion of Science; Grant number: 16000326; Grant sponsor: Ministry of Education, Culture, Sports, Science and Technology of Japan; Grant number: A14; Grant sponsor: Primate Research Institute, Kyoto University; Grant numbers: 4-1 (2004), 3-1 (2005), and 1-6 (2006).

*Correspondence to: Takeshi Nishimura, D.Sc., Primate Research Institute, Kyoto University, Kanrin, Inuyama, Aichi 484-8506, Japan. E-mail: nishimur@pri.kyoto-u.ac.jp

Received 24 July 2006; accepted 17 August 2007

DOI 10.1002/ajpa.20719
Published online 25 October 2007 in Wiley InterScience (www.interscience.wiley.com).

as seen in humans to be absent from nonhuman primates (Negus, 1949; Lieberman, 1984; Laitman and Reidenberg, 1993), and the term "descent" of the larynx or hyoid often implies the nonuniform changes of human SVT. However, despite their SVT configuration in adults, chimpanzees also show a great descent of the larynx with the descent of the epiglottis from the velum, as in humans (Nishimura et al., 2003, 2006). On the other hand, the face grows to be projected and prognathic in adults, to allow for a great elongation in the oral cavity and tongue in chimpanzees (Nishimura et al., 2006). These facts strongly suggest that the SVT configuration unique to humans arose along with evolutionary trends in face flattening in the human lineage and did not involve the great descent of the larynx (Nishimura et al., 2006). However, uncertainty remains regarding the evolutionary path of the two processes involving the great descent of the larynx before the divergence of the human and chimpanzee lineages.

Laryngeal descent in humans causes some modifications to the integrated functions of the pharyngeal region, including swallowing, breathing, and vocalization. In humans, the epiglottis descends to lose contact with the velum, following modification to the epiglottic movements required for swallowing (Sasaki et al., 1977). This adult mode is achieved by the approximation of the laryngeal skeleton to the hyoid (Ekberg, 1982; Ekberg and Sigurjónsson, 1982; Vandaele et al., 1995; Reidenbach, 1997). The descent of the laryngeal skeleton from the hyoid, weakening the physical linkages between them, is probably one prerequisite for such movements (Nishimura, 2003). On the other hand, the SVT is involved in the resonance of the sound sources generated by the vocal folds of the larynx to generate vowel-like sounds, which form one basis for vocal communication (Fant, 1960; Lieberman and Blumstein, 1988; Titze, 1994; Stevens, 1998). Humans use sequential and rapid modifications of the SVT topology to produce a wide range of formant patterns and transitions. Although the nonhuman primates also share such faculties *per se* (Fitch, 2000b; Riede et al., 2005), the great descent of the larynx as seen in humans might contribute to the productions of distinct formant patterns, with extensive modifications to the pharyngeal topology (Lieberman et al., 1969) or it might enhance the sophisticated modifications of the SVT topology for the fluent production of speech sounds (Fitch, 2000b). In fact, laryngeal descent in humans is accompanied by the development of a unique tongue anatomy with equally vertical and horizontal dimensions (Crelin, 1987; Zemlin, 1988), resulting in the rearrangement of the internal musculature of the human tongue to make its surface highly mobile (Takemoto, 2001).Thus, an understanding of the evolutionary path of the two developmental processes of the laryngeal descent will shed light on the evolution of the anatomical foundations for human faculties of feeding and vocal behaviors.

Here, we used magnetic resonance imaging (MRI) to study the developmental changes in the spatial configuration of the hyoid, laryngeal skeleton, epiglottis, velum and palate in the first three years of life in living Japanese macaques. The development of laryngeal descent was compared with that reported for living humans (Lieberman et al., 2001) and chimpanzees (Nishimura et al., 2003, 2006), for examining the presence or absence of the two developmental processes involving the great descent of human larynx in macaques and their contributions to the developmental changes in pharyngeal topology. We will use these observations to discuss the evolutionary path of the great descent of the larynx as seen in humans and chimpanzees, with functional backgrounds of feeding and vocalization.

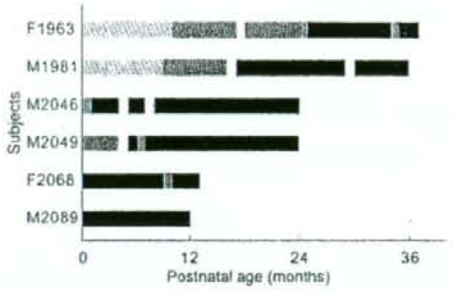

Fig. 1. Longitudinal sample of data used in this study. Black boxes indicate the magnetic resonance (MR) images used. Slash boxes, gray boxes, and spaces indicate axial, poor-quality, and missing MR images, respectively. They are not used for the analyses. M and F before the subject number indicate the subject sex of male and female, respectively.

METHODS

Subjects

We examined the development of the pharyngeal anatomy in six Japanese macaques, *Macaca fuscata*, using a semilongitudinal sample of two females and four males (see Fig. 1). The care and use of the subjects conformed to the guidelines of the Primate Research Institute (PRI) of Kyoto University (2002). Two monkeys were born at the PRI during each birth season in 2003, 2004, and 2005, and were examined over the first three, two, and one years of their life, respectively (see Fig. 1).

Imaging procedures

The heads and necks were scanned using the same General Electrics Signa Profile MRI scanner (0.2 T) at the PRI, with the same extremity receiving-coil, every month from one month of age (see Fig. 1). The examinations were set up primarily for another study on the developmental changes of brain structures. The subjects were anesthetized intramuscularly with a mix of 4.0 mg ketamine hydrochloride (Sankyo, Tokyo, Japan) and 0.15 mg medetomidine hydrochloride (Meiji Seika Kaisha, Tokyo, Japan) per kilogram of body weight. After the MRI examinations, the subjects were woken with a solution of 0.75 mg atipamezole hydrochloride (Meiji Seika Kaisha) per kilogram of body weight. During scanning, they were placed prostrate and fixed to the same receiving coil using a custom cephalostat (Fig. 2A,B), in which their heads were raised (Fig. 2B). The subjects examined in this study were in a different posture from those subjects in the comparable studies of chimpanzees (Nishimura et al., 2003, 2006) and humans (Lieberman et al., 2001). The scans were taken with sagittal or axial three-dimensional spoiled gradient recalled acquisition in the steady state (3D-SPGR; Fig. 1). They were taken with time-to-echo durations of 9 ms, time-to-repeats of 44 ms, 1.5 mm slice thickness, an acquisition matrix of 256 × 256, and with one excitation. The fields of view of 12 or 15 cm

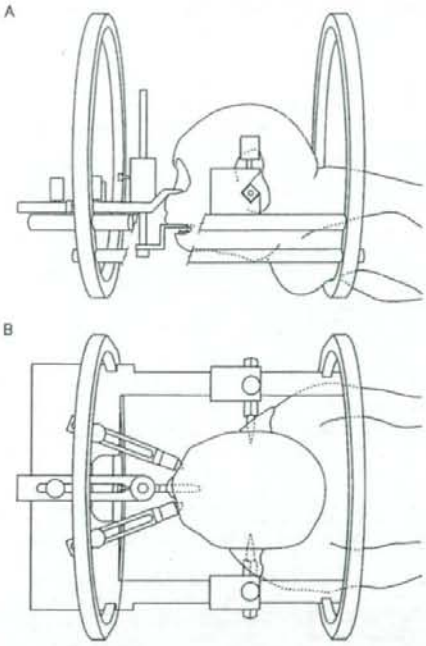

Fig. 2. Schema of the custom cephalostat used in the present study. **A**, left lateral view. **B**, top view. The subjects were always fixed to the cephalostat, using bars placed into each ear canal, bars holding the inferior edge of each orbit, and a bar holding the incisors. The animals were always placed prostrate and their head was raised to retroflex the neck.

were chosen based on subject size (see Appendix). The imaging protocol was approved by the Ethics Panel of the PRI. The matrix of all MR images was 256 × 256 pixels and image resolutions ranged from 0.47 × 0.47 or 0.59 × 0.59 mm/pixel (see Appendix). The following analyses included the sagittal scans and we took care to exclude any scans obscured by artifacts decreasing the accuracy of the measurements (see Fig. 1).

Measurements

MR images were transferred from the MRI scanner to a personal computer, using Vox-Base Transmit software (J-Mac System, Sapporo, Japan). The images transferred were converted from DICOM to TIFF format, using IrfanView software (version 3.91, available on http://www.irfanview.com/). Images were analyzed from a three-way set of images reformatted using Amira software (version 3.1, TGS, San Diego, CA) to record measurement points and standard planes using Adobe PhotoShop CS software (version 1.0, Adobe Systems, San Jose, CA). The pixel-based landmarks for linear dimensions were identified and the coordinate values were measured three times from MR images, using ImageJ software (version 1.32i, available on http://rsb.info.nih.gov/ij/). If the values were inconsistent, they were re-identified. This procedure makes the measurement value independent of any error accompanied with identifications of the landmarks, in contrast to procedures using calipers where the landmarks and dimensions were simultaneously identified and measured. It should be noted that this procedure inevitably provides an error dependent on the spatial resolution of an image, at largest a measurement plus or minus the diagonal length of a pixel size: 0.66 mm or 0.83 mm in this study.

For comparisons with measurements reported in humans (Lieberman et al., 2001) and chimpanzees (Nishimura et al., 2003, 2006), measurement points and standard planes on the midsagittal plane included the following: anterior nasal spine (ANS), anterior tubercle of the atlas (ATA), endoprosthion (EPr), hyoid bone (HB), posterior nasal spine (PNS), posterior oropharyngeal wall (POW), palatal plane (PP), posterior pharyngeal wall line (PPW), and vocal fold (VF). These definitions (Table 1) are those that have been used for chimpanzees (Nishimura, 2005; Nishimura et al., 2006) and are roughly equivalent to those used for radiographic studies of humans (Lieberman et al., 2001). We used two additional points, epiglottis (EG) and velum (VL). These definitions (given in Table 1) were those used for chimpanzees (Nishimura et al., 2003, 2006). Measurements included the length of the oral cavity (hereafter SVT_H length, as customary), along the EPr-ATA line from the EPr to the POW; the length of the pharyngeal cavity (hereafter SVT_V length, as customary) parallel to the PPW from the VF to the PP; the distances from the hyoid to the palate and to the vocal folds (HB-PP and HB-VF, respectively), parallel to the PPW from the HB to the PP and to the level of VF (see the keys to Fig. 3A). These definitions of dimensions are those used for chimpanzees by Nishimura (2005) and Nishimura et al. (2006) and are similar to those used for humans by Lieberman et al. (2001). Although, there are some differences in the abbreviations of some measurement points and planes, the dimensions are the same as those used for the chimpanzee by Nishimura et al. (2003). We also examined the lengths of the oropharyngeal (op) and laryngopharyngeal (lp) parts of the vertical pharyngeal cavity, parallel to the PPW from the EG to the levels of the VL and VF, respectively (see the key to Fig. 3A). These dimensions are the same as those used by Nishimura et al. (2003, 2006), but there are no comparable measurements in humans (Lieberman et al., 2001).

Comparable growth stages

In this study, measurements were recorded for the Japanese macaques at chronological ages ranging from one month to three years (present study), and compared with those for chimpanzees from four months to five years (Nishimura et al., 2003, 2006) and for humans from one month to 13 years and nine months (Lieberman et al., 2001). The developmental trajectories were here compared in terms of the developmental ages of the three species after their chronological ages had been adjusted to correspond to dental eruption stages, which reflect legitimately comparable growth phases. In the present study, three growth stages were defined following Nishimura et al. (2006): "early infancy," "late infancy," and "juvenile." These comprised the dental stage from birth to before the eruption of the deciduous dentition, the stage from the eruption of the deciduous dentition to before the eruption of the first molars, and the stage after the eruption of the first molars and before the eruption of the second molars, respectively.

TABLE 1. Definitions of the measurement points and standard planes used

Landmarks and planes	Abbreviations	Definition
Anterior nasal spine	ANS	The most anterior inferior point of the piriform aperture of the nose, which is roughly equivalent to the most anterior root point of the nasal septum[a]
Anterior tubercle of the atlas	ATA	The superior-inferior midpoint of the anterior tubercle of the atlas[b]
Epiglottis	EG	The most superior point of the epiglottis
Endoprosthion	EPr	The most anterior inferior point of the lingual surface of the premaxilla alveolar
Hyoid bone	HB	Most anterior and superior point of the insertion of the geniohyoid muscle onto the hyoid bone
Posterior nasal spine	PNS	The most posterior point of the maxillary body at the level of the nasal floor at the junction of the hard and soft palates
Posterior oropharyngeal wall	POW	Point on the posterior pharyngeal wall opposite the anterior tubercle of the atlas along the plane from EPr to ATA
Palatal plane	PP	The line from the ANS to PNS
Posterior pharyngeal wall	PPW	The most posterior straight line of the pharyngeal wall from the level of the velum to the laryngeal orifice
Vocal folds	VF	The anterior–posterior midpoint of the vocal folds
Velum	VL	The most posterior inferior point of the palatine velum, excluding the uvula

All landmarks and planes were defined on the mid-sagittal plane of the MR images.

[a] This definition is the same as that for chimpanzees used by Nishimura (2005) and Nishimura et al. (2003, 2006), but is different from that used by Lieberman et al. (2001) in the narrow sense because no true anterior nasal spine is found in Japanese macaques and chimpanzees.

[b] This definition is the same as that used for chimpanzees by Nishimura (2005) and Nishimura et al. (2003, 2006), but is different from that used for the human ATA (Lieberman et al., 2001). The human ATA is defined as the most anterior and superior point of the anterior tubercle of the atlas that projects on the sagittal plane in radiographs. This point was identified only obscurely on mid-sagittal MR images of Japanese macaque and chimpanzee subjects, so the nonhuman primate ATA was here redefined as being roughly equivalent to the human ATA.

On the basis of studies of dental eruption ages in a cross-sectional sample of Japanese macaques (Iwamoto et al., 1984, 1987), captive living chimpanzees (Conroy and Mahoney, 1991; Kuykendall et al., 1992), and humans of European origin (Hurme, 1949; Lysell et al., 1962; Smith and Garn, 1987; Smith, 1991), the chronological ages of the three species were adjusted to correspond to dental stages. In Japanese macaques, "early infancy" (Fig. 3B) is defined here as the period from birth to eight months of age, "late infancy" (Fig. 3C) as the period from eight months to one year and eight months of age, and the "juvenile" stage (Fig. 3D) as that period from one year and eight months to three years and eight months of age (see Fig. 4). The definitions for chimpanzees and humans used here follow those by Nishimura et al. (2006). In chimpanzees, "early infancy" is defined as the period from birth to one year of age, "late infancy" as the period from one to three years of age, and the "juvenile" stage as that period from three to seven years of age. For humans, "early infancy" is defined as the period from birth to two and half years of age, "late infancy" as the period from two and half to six years of age, and the "juvenile" stage as that period from six to 12 years of age (see Fig. 4). Thus, in this study, the developmental patterns were examined up to two years and eight months of age in Japanese macaques, up to five years in chimpanzees, and up to nine years in humans; in the "early infancy," "late infancy," and early "juvenile" stages (see Fig. 4). In Figures 6–8, mean values for pooled sex measurements have been recalculated for any given category of chronological age for chimpanzees (Nishimura et al., 2003, 2006) and humans (Lieberman et al., 2001).

Comparability of the measurements

It should be noted that the position of the hyoid and larynx relative to other structures can only be compared accurately under equivalent conditions (Fitch and Giedd, 1999; Lieberman et al., 2001; Nishimura et al., 2006). Human subjects were recorded in an upright position during quiet respiration using lateral radiographs (Lieberman et al., 2001), whereas the subjects of the chimpanzee and Japanese macaque were recorded in the supine and prostrate position, respectively, under general anesthesia using MRI (Nishimura et al., 2003, 2006; present study). In addition, the jaw was allowed to open by its own weight (see the MR image in Fig. 3B–D). These varied head and mouth postures might alter the conformation of the living subjects and thereby affect the measurements in different ways for the three species. A study with embalmed specimens of chimpanzees (Nishimura, 2005) indicated that head posture has many potential influences on measurements of those dimensions defined by the landmark of the HB, although it has small influences on the other dimensions defined in this study. Such risks were re-evaluated in this study with comparisons of measurements taken with MRI scans at the prostrate and supine position in the same subject (macaque number 1963), at 43 months of age (see Results). In addition, anesthesia might have had an influence on conformation. Such methodological differences limit accurate comparisons between the absolute values of dimensions measured in the three species. Nevertheless, the subjects were always recorded using the same conditions and procedures in each species, so the degree of any deformity presumably would be consistent in each subject. Thus, this study was mainly concerned with comparing developmental trajectories of the dimensions, using the increases of the measurement values in comparable growth stages, rather than with attempting to define any absolute values of the dimensions and ratios among the three species.

Of semilongitudinal sample of the six Japanese macaques, changes of dimensions in early infancy were calculated using the means of the measurements at two

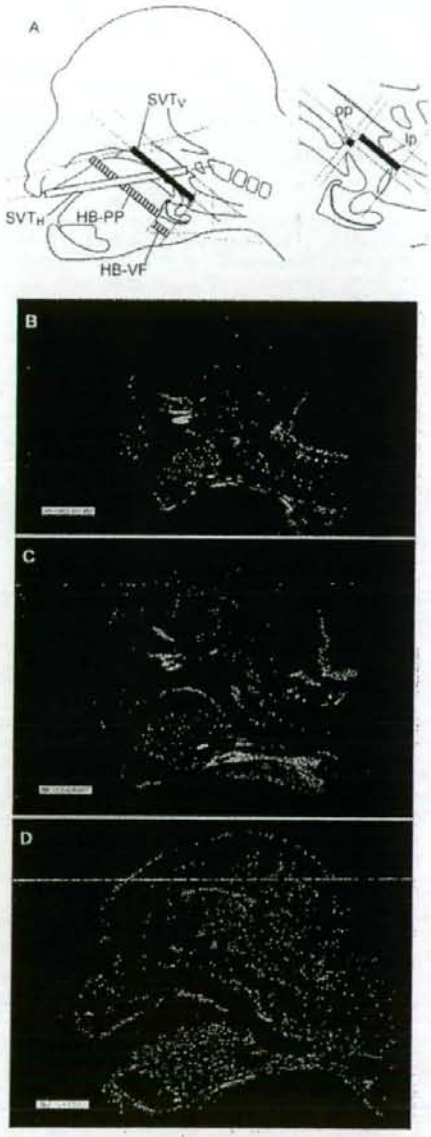

Fig. 3. Growth of the SVT in Japanese macaques, *Macaca fuscata*. **A**, Left: midsagittal diagram of SVT_H (outlined), SVT_V (filled) lengths, and the distances from the hyoid to the vocal folds (HB-VF, dotted) and to the palate (HB-PP, dotted). Right: enlarged diagram of the oropharyngeal (op) and laryngopharyngeal (lp) dimensions. See Subjects and Methods for definitions of the dimensions. **B–D**, Midsagittal MR images at one month of age in a male subject (B; no. 2089); 13 months of age in a male (C; no. 2049); and 25 months of age in a male subject (D; no. 1981). Scale bar = 2.0 cm.

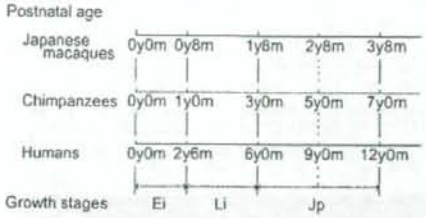

Fig. 4. Analogous growth stages (early infancy, late infancy, and juveline period) in Japanese macaques, chimpanzees, and humans. The chronological ages of the species are expressed in terms of dental stages, based on the dental eruption ages. The dotted line exemplifies the comparisons made of 2 years and 8 months old Japanese macaques to 5-year-old chimpanzees and 9-year-old humans.

months and eight (or nine) months of age for subject numbers 2049, 2068, and 2089; in late infancy with means in nine months and one year and eight months of age for subject numbers 2046 and 2049; and in the early juvenile period with the measurements in one year and nine months and two year and eight months of age for subject number 1981.

RESULTS

The position of the subjects on the scanner table had dominant influences on the head and neck posture. Figure 5 shows that the neck of all the subjects was always retroflexed sharply at the level below the vocal folds and the pharynx was angled relative to the head and oral cavity at the supine (Fig. 5A) more than at the prostrate position (Fig. 5B). The mouth was almost closed at the supine position. Such deformities have a profound influence on the distance from the hyoid to the palate, although they have a limited effect on the measurements in the other dimension. The HB-PP dimension at the supine position decreased by 19% of the measurement at the prostrate position (Table 2). However, the other dimensions, excluding the oropharyngeal (op) parts, changed in length at the supine position by increase or decrease of less than 5% of the measurements at the prostrate (Table 2). The op showed a increase at the supine by 38% of the measurements at the prostrate position, but this decrease of 0.02 cm was less than the pixel size of the images (Table 2). The spatial relationship of the velum to the epiglottis was almost unchangeable, although the configuration of the velum was slightly modified by head position (Fig. 5A,B). Thus, all dimensions used in this study were affected to varying degrees by the head posture, and comparisons using absolute values have not been addressed in the discussion.

In these Japanese macaques, the SVT_H increased in length at a rate similar to the SVT_V during early infancy, but thereafter the SVT_H showed slightly greater growth relative to that of the SVT_V. This is reflected in the age-related changes in the ratio of the SVT_H to SVT_V lengths as shown in Figure 6A and Appendix. Although the absolute values varied at the same age between the subjects examined here, this ratio was almost constant in early infancy and increased slightly after late infancy: increases from 1.84:1 to 1.85:1 in early infancy, from 1.97:1 to 2.08:1 in late infancy, and from 1.88:1 to 1.98:1 in the early juvenile stage. In contrast,

the ratio decreases during early infancy from 2.22:1 to 1.89:1 in chimpanzees (Nishimura et al., 2003) and from 1.47:1 to 1.25:1 in humans (Lieberman et al., 2001). Thereafter, although the ratio decreases consistently to reach the adult ratio of 1:1 by nine years of age in humans (Lieberman et al., 2001), an age-related trajectory similar to that in the Japanese macaques is seen in chimpanzees with increases to 2.10:1 at the end of the early juvenile stage (Nishimura et al., 2006). In Japanese macaques, the SVT_H and SVT_V grew constantly in the first three years of life, with the former growing at a faster rate than the latter after late infancy. Figure 6B and Appendix show that the SVT_H length increased constantly in each subject. It is reflected by the constant ratio increases of 1.2-, 1.2-, and 1.1-fold in the three stages, respectively; increases from 4.0 cm to 4.9 cm in the early infancy, from 4.9 cm to 5.9 cm in the late infancy, and from 6.1 cm to 7.0 cm in the early juvenile stage. Although the absolute dimensions are always much longer than that in the Japanese macaques, the documented SVT_H in chimpanzees shows a very similar growth trajectory: increases of 1.1-, 1.3-, and 1.2-fold in the three stages, respectively (Fig. 6B; Nishimura et al., 2003, 2006). The human SVT_H shows a similar growth trajectory to the two other species in early infancy, but thereafter it grows much more slowly: increases of 1.2-, 1.0-, and 1.0-fold in the three stages, respectively (Fig. 6B; Lieberman et al., 2001). This difference after late infancy means that the absolute SVT_H length in Japanese macaques reached that of humans in the juvenile period (Fig. 6B). Figure 6C and Appendix show that the SVT_V length increased constantly in each subject of Japanese macaques, although the absolute dimensions varied. It is reflected by the constant ratio increases of 1.2-, 1.1-, and 1.1-fold in the three stages, respectively: increases from 2.2 cm to 2.6 cm in the early infancy, from 2.5 cm to 2.8 cm in the late infancy, and from 3.2 cm to 3.6 cm in the early juvenile stage. The documented SVT_V in humans and chimpanzees grows more rapidly than that in Japanese macaques in early infancy: increases of 1.5-fold in chimpanzees (Nishimura et al., 2003) and 1.4-fold in humans (Lieberman et al., 2001), respectively. However, growth slows thereafter and the trajectories are almost similar to those seen in the Japanese macaques: increases of 1.2-fold in late infancy and of 1.2-fold in the early juvenile period in chimpanzees (Nishimura et al., 2003, 2006); 1.2-fold in late infancy and of 1.2-fold in the late juvenile period in humans (Lieberman et al., 2001). This difference means that in the initial phase of early infancy, the absolute dimension of the SVT_V in chimpanzees is almost similar to that in Japanese macaques, but the rapid growth in chimpanzees in early infancy causes a divergence in absolute dimensions (Fig. 6C).

As for the growth of the SVT_V, in Japanese macaques the laryngeal skeleton descended negligibly relative to the hyoid, so the configuration of the hyolaryngeal complex remained unchanged during the first three years. This is documented in Figure 7A and Appendix. The

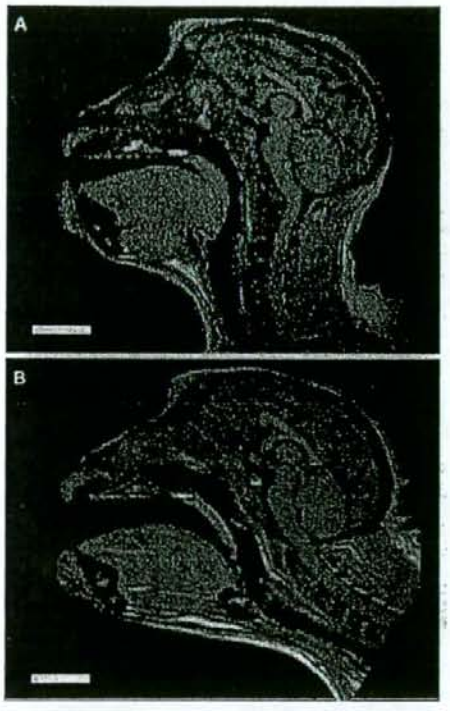

Fig. 5. MR images in the supine (**A**) and prostrate (**B**) positions. Both scans were taken in a same subject no. 1963, at 43 months of age. The neck is angulated at the supine more than at the prostrate position. The configuration of the velum is modified, but the spatial relationship between the velum and epiglottis changes minimally. Scale bar = 2.0 cm.

TABLE 2. Comparisons of the measurements in prostrate and supine positions

Posture	FOV (mm)	Pixel sizes (mm/pixel)	SVT_H (cm)	SVT_V (cm)	HB-PP (cm)	HB-VF (cm)	Op[a] (cm)	Lp (cm)
Prostrate	150	0.59	7.06	3.70	3.95	0.75	0.04	1.60
Supine	150	0.59	6.72	3.59	3.18	0.76	0.05	1.54
Difference of the measurements[b]			−0.34	−0.11	−0.76	0.02	0.02	−0.06
Ratio of the difference relative the measurements at the prostrate position[b]			−5%	−3%	−19%	2%	38%	−4%

The dimensions were measured at the prostrate and supine postures in a same subject no.1963, at 43 months of age. See Methods for abbreviations of the dimensions.

[a] This dimensions increased 38% longer at the supine than at the prostrate position, but the measurements are under the spatial resolution of the image.

[b] There are some rounding errors.

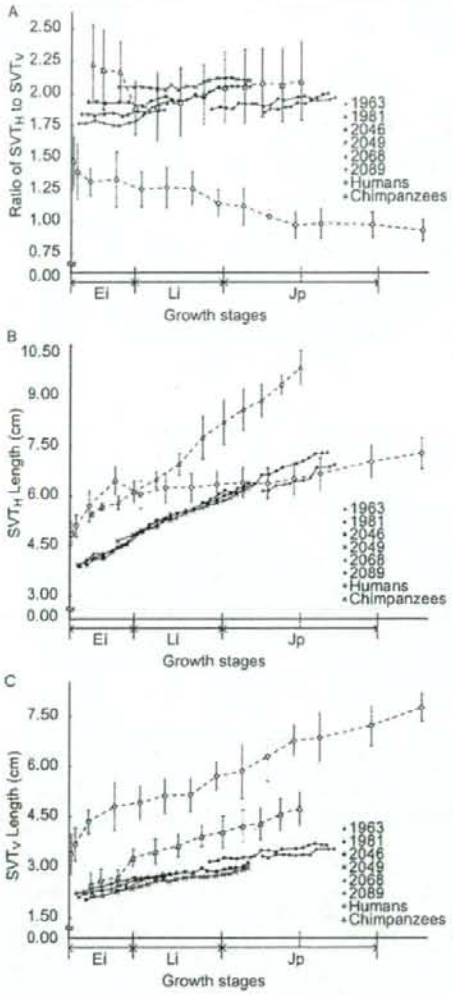

Fig. 6. Growth of the SVT in the six Japanese macaques studied. **A**, Age-related changes in the ratio of SVT_H to SVT_V lengths. **B**, Growth of the SVT_H lengths. **C**, Growth of the SVT_V lengths. Measurements on chimpanzees (pooled sexes, open triangles) and humans (pooled sexes, open circles), respectively, with permission. The growth stages and their abbreviations are in accordance with those in Figure 4.

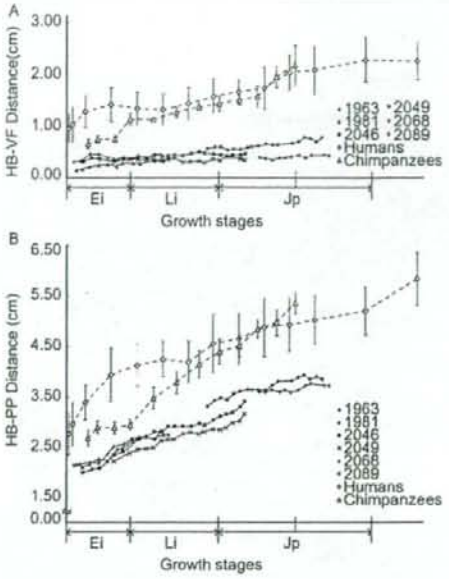

Fig. 7. Increases in the dimensions of the SVT_V. **A**, Distance from the hyoid to the vocal folds (HB-VF). **B**, Distance from the hyoid to the palate (HB-PP). Measurements on chimpanzees (pooled sexes, open triangles) and humans (pooled sexes, open circles), respectively, are from Nishimura et al. (2003, 2006) and Lieberman et al. (2001) with permission. The growth stages and their abbreviations are in accordance with those in Figure 4.

distance from the hyoid to the vocal fold (HB-VF) showed only a negligible change during the period evaluated: an increase of 0.43 cm from 0.28 cm to 0.71 cm. By contrast, the laryngeal skeleton descends rapidly in early infancy and thereafter continues to descend gradually in both humans (Fig. 7A; Lieberman et al., 2001) and chimpanzees (Fig. 7A; Nishimura et al., 2003, 2006). On the other hand, in these Japanese macaques the hyoid descended negligibly relative to the palate in the initial phase of early infancy and thereafter descended gradually. This growth pattern is reflected in the growth changes in the distance from the hyoid to the palate (HB-PP) documented in Figure 7B and Appendix. The HB-PP increased negligibly from 2.10 to 2.19 cm in the first four months of life, but thereafter it increased constantly to 3.90 cm: an increase of 1.8-fold. Such a growth trajectory is seen in chimpanzees (Fig. 7B; Nishimura et al., 2003, 2006), despite a difference in the timing of its initiation. The distance increases negligibly in early infancy and thereafter increases 1.8-fold by the end of the early juvenile phase. Although the human hyoid descends relative to the palate even in early infancy, it continues to descend after late infancy: a total increase of 1.8-fold (Fig. 7B; Lieberman et al., 2001). Nevertheless, in these Japanese macaques, the epiglottis descended negligibly from the velum even after late infancy, and so the oropharyngeal component remained small. This is reflected in Figure 8A and Appendix, demonstrating that the oropharyngeal component (op) remained short compared with an increase of this dimension in chimpanzees: 2.6-fold increase from 0.11 to 0.29 cm in the first three years of Japanese macaques and an increase of 6.0-fold in the first five years of life in chimpanzees. On the other hand, the laryngopharyngeal component (lp), caudal to the oropharyngeal component, lengthened constantly as in chimpanzees, despite smaller absolute dimensions: 1.9-fold increase from 7.88 to 15.20 cm in the first three years of life in Japanese macaques, and an increase of 2.1-fold in chimpanzees

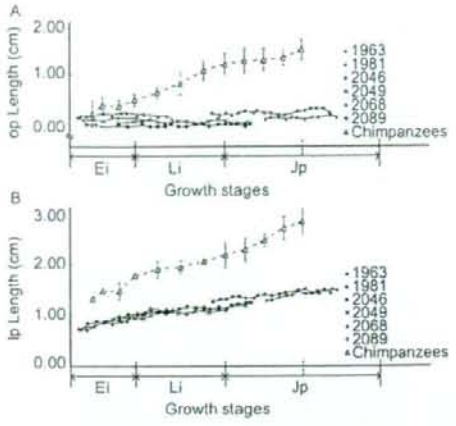

Fig. 8. Growth in the pharyngeal dimensions. **A**, Length of the oropharyngeal part (op). **B**, Lengh of the laryngopharyngeal part (lp). Measurements on chimpanzees (pooled sexes, open triangles) are from Nishimura et al. (2003, 2006) with permission. Measurements on humans were not provided in Lieberman et al. (2001). The growth stages and their abbreviations are in accordance with those in Figure 4.

(Fig. 8B and Appendix). Thus, there were negligible descents of the laryngeal skeleton relative to the hyoid and of the the epiglottis relative to the velum, although there was somewhat greater descent of the hyoid relative to the palate. In fact, the great descent of the larynx relative to the palate is accounted for by the distance between the hyoid and laryngeal skeleton, but not by that between the hyoid and palate.

DISCUSSION

This study provides evidence supporting the idea that nonhominoid primates do not share full laryngeal descent as seen in humans and chimpanzees. Here, Japanese macaques showed a negligible descent of the laryngeal skeleton relative to the hyoid, whereas they showed the descent of the hyoid relative to the palate as seen in chimpanzees. The developmental descents of the larynx and hyoid relative to the palate have been shown by a computer tomography (CT) study using a mixed sample with longitudinal- and cross-sectional ontogenetic series of living long-tailed and rhesus macaques, *Macaca fascicularis* and *M. mulatta* (Flügel and Rohen, 1991), although the epiglottis maintains contact with the velum to restrict the pharyngeal cavity from facing the movable tongue in macaque monkeys (Laitman et al., 1977; Flügel and Rohen, 1991). Unfortunately, the discrepancy in definitions and the scarcity of the measurements reported by those authors prevent direct comparisons with the detailed studies of humans (Lieberman et al., 2001) and chimpanzees (Nishimura et al., 2003, 2006). Nevertheless, another anatomic study showed a distinction in adult anatomy of the hyolaryngeal complex between hominoids and the other anthropoids (Nishimura, 2003). In adult hominoids, including humans, the laryngeal skeleton is lowered from the hyoid and is assured of mobility independent of the hyoid. This contrasts with the other anthropoids, where the laryngeal skeleton is locked onto the hyoid body and is tied tightly with or directly articulated with the greater horn of the hyoid. Such a distinction between hominoids and the other anthropoids strongly supports the present finding of a negligible descent of the laryngeal skeleton relative to the hyoid. In addition, this study suggested that such a negligible descent in part contributes to the lack of the descent of the epiglottis from the velum in Japanese macaques, forming the oropharyngeal region. Thus, the evolutionary modifications to the development in the hyolaryngeal complex probably enhanced the descent of the epiglottis from the velum, establishing the great descent of the larynx in a common ancestor of extant hominoids.

The developmental descent of the hyoid was shared by these Japanese macaques, although this descent probably makes little contribution to the descent of the the epiglottis from the velum. Despite slight differences in the timing and rate, chimpanzees show descent of the hyoid analogous to that in humans (Nishimura et al., 2006). However, the other nonhuman primates are believed not to share it (Lieberman, 1984; Laitman and Reidenberg, 1993; Fitch, 2000a; Nishimura et al., 2006), because no such descent of the epiglottis has been detected in them (Negus, 1949; Laitman and Reidenberg, 1993; Fitch, 2000b). It is to be noted that there are slight differences in the timing of the hyoid descent in humans versus that seen in chimpanzees and macaques. This might be caused by the development of the laryngeal air-sac in the latter two species. Whereas humans have no sac, chimpanzees and macaques have one passing between the hyoid and the thyroid cartilage (Starck and Schneider, 1960; Hayama, 1970; Hewitt et al., 2002). This sac develops to reach the dorsal aspect of the body of the hyoid as early as four months of age in chimpanzees (Nishimura et al., 2007) and even at one month of age for Japanese macaques (present study). The associated anatomical changes might thereby contribute to elevate the hyoid additionally in early infancy (Nishimura et al., 2006). On the other hand, the developmental trajectory of the descent of the hyoid relative to the palate in humans was evaluated using averaged dimensions of a semilongitudinal sample (Lieberman et al., 2001). This might cancel out the developmental trajectory as seen in chimpanzees and macaques: i.e., the delayed beginning of the hyoid descent. Despite being a case report for only one male subject, one study on a human infant showed that the position of the hyoid is unchanged relative to the palate in the initial phase of early infancy (Vorperian et al., 1999). This issue must be resolved using a large longitudinal sample. However, despite slight differences, the descent of the hyoid as seen in humans must have arisen before the divergence of the extant hominoid and the cercopithecoid lineages.

The SVT_H is slightly decreased in length at the supine relative to that at the prostrate position. Such a decrease is caused by the more acute angle of the neck, which moves the PPW anterior. Among the dimensions along the neck, the HB-PP was significantly influenced by head posture. The dimensions in the neck were all defined as linear dimensions parallel to the PPW. The hyoid is tightly linked to the mandible by the geniohyoid and myohyoid muscles, ligaments, and membranes (Crelin, 1987; Zemlin, 1988; Williams, 1995). Anatomically, the position of the hyoid is affected by the position of the mandible rather than the pharyngeal wall. In contrast, the vocal folds are included within the laryn-

geal skeleton, which is tightly linked to the pharyngeal wall by the pharyngeal constrictors (Crelin, 1987; Zemlin, 1988; Williams, 1995). Therefore, the position of the VF does not change significantly relative to the PPW. Moreover, the VF is close to, and the HB distant from, the PPW. This indicates that the more obtuse angles of the neck relative to the head move the intersection point forward between the PP and the line parallel to PPW from HB, to extend the HB-PP dimension. Such differences in anatomy probably underlie that the HB-PP dimension is most sensitive to head posture, in contrast to the SVT_V and HB-VF. The epiglottis is attached to the laryngeal skeleton and therefore the position of the epiglottis relative to the pharynx is less sensitive to head posture, as seen in that of vocal fold. This probably contributes to the unchangeable spatial relationship of the velum and epiglottis (op), despite modifications in the velum conformation. Thus, the head and mouth postures at scanning affect the position of the hyoid relative to the palate (HB-PP), while they have limited influence on the spatial relationship of the laryngeal skeleton and hyoid (HB-VF). Although such artifacts prevent a direct and statistical comparison of the absolute values of the HB-PP measure in the three species, this study showed a steady elongation in this dimension for each subject, indicating a similar growth trajectory among the three species. This does not prevent the interpretation that the developmental descent of the hyoid in Japanese macaques is analogous to the descent in chimpanzees, even though there may be some overestimations of this dimension.

There were varying absolute dimensions at any given point among subjects in this study, although the growth trajectory—the slope—of the dimensions almost coincided during the same growth phase among the subjects. This variation was probably caused by intersubject variations of each dimension and was not induced by possible irregularities in the MRI procedure or by variations in the motions of the animals during measurement. Juvenile females were slightly smaller than males for all measurements. Although this may show the sexual dimorphism that develops as the animals grow, this issue has to be resolved in future studies using a larger sample.

There is still uncertainty about the evolutionary advantages of the descent of the laryngeal skeleton relative to the hyoid. This descent may contribute to the physical foundations for a prerequisite for speech production based on highly independent regulations in the activities of the laryngeal skeleton for generating sound sources, and in hyoid activities for tongue motions in articulation (Nishimura et al., 2003; Nishimura, 2006). However, it is likely that it originally conferred advantages for functions unrelated to the sophisticated articulation of modern speech. The hyolaryngeal complex plays an important role in integrated functions of the pharynx and larynx, such as swallowing, breathing, and vocalization (Negus, 1949; Lieberman, 1984; Crelin, 1987; Zemlin, 1988; Williams, 1995; Hiiemae and Palmer, 1999, 2003). This indicates that the descent of the laryngeal skeleton relative to the hyoid might have arisen independently to facilitate some of these integrated functions. Anatomically, this descent has a minor influence on the dimension of the pharynx. In fact, despite the absence of this descent, the descent of the hyoid relative to the palate produces a growth trajectory of the SVT_V similar to that in chimpanzees and humans after late infancy in Japanese macaques. However, the present study showed that the presence or absence of this descent differentiates the pharyngeal configuration in humans and chimpanzees from that in Japanese macaques: this descent accompanies the descent of the epiglottis from the velum in the former two species. This finding strongly suggests that the developmental modifications to the dynamic activities and physiological performance of the hyolaryngeal complex and epiglottis during the early infancy of hominoids will provide valuable insights into the original functional adaptations of this descent. Although there is little such information in nonhuman primates, in humans the epiglottis descends to lose contact with the velum at about six months of age and this anatomical development follows modification to the epiglottic movements in swallowing (Sasaki et al., 1977). The descent of the laryngeal skeleton relative to the hyoid may also provide anatomical foundations for the modified movement of the human epiglottis (Nishimura, 2003). Although there is controversy regarding the activity of the epiglottis during swallowing, it contributes to separate the respiratory and swallowing pathways in all nonhuman mammals (Laitman et al., 1977; Larson and Herring, 1996; Crompton et al., 1997). It will be necessary to study the developmental changes in the activities of the hyolaryngeal complex and its effects on the epiglottic movements in swallowing during the early infancy of hominoids and the other anthropoids. Such studies will contribute to our understanding of the selective advantages of this descent in a common ancestor of extant hominoids.

Unlike the descent of the laryngeal skeleton, the evolutionary path of the descent of the hyoid is yet to be evaluated. This descent is probably a morphological consequence of mandibular growth. The hyoid is linked tightly to the mandible by muscles, ligaments, and membranes (Zemlin, 1988; Williams, 1995), and this anatomical restriction possibly maintains the spatial relationship between the two. In fact, in humans, the hyoid descends along with the superior–inferior growth of the mandibular ramus (Lieberman and McCarthy, 1999; Lieberman et al., 2001). Such an anatomical linkage is likely in nonhuman primates (Swindler and Wood, 1973; Ankel-Simons, 2000), and most nonhuman primates probably share this anatomical pathway in growth. This suggests that this descent may have originally conferred little inherent selective advantage. However, the hyoid also provides a base for the tongue musculature, so its activities have a major role in tongue movements (Zemlin, 1988; Williams, 1995; Hiiemae and Palmer, 2003). These features associated with the hyoid underlie the coordinated cyclic activities of the jaw and tongue in each phase of feeding behavior as seen in humans and macaques, and such activities are varied by the physical nature of the foods and liquids being swallowed (Hiiemae et al., 1995; Hiiemae, 2000; Hiiemae et al., 2002; Hiiemae and Palmer, 2003). This suggests that hyoid descent may alter the coordinated activities, along with some modifications to feeding behavior. On the other hand, this descent might also modify the activities of the hyoid in vocalization and speech. During human vocalization, the hyoid is shifted anterior to the region used in feeding to widen the pharyngeal cavity and moves steadily and rapidly to produce a fluent sequence of speech sounds, although it moves in a constrained region compared with the case in feeding (Hiiemae et al., 2002; Hiiemae and Palmer, 2003). In contrast, a distinct lowering of the hyoid has been found to lengthen the pharyngeal cavity in some mammals, including nonhuman primates, but little in the way of further sophisticated movements can be detected (Fitch, 2000b; Fitch and Reby, 2001). Such a difference might be

attributed to the presence or absence of a hyoid descent analogous to that in humans. The nonhuman primates lower the larynx temporarily and modify the tongue topology to produce a wide range of formant patterns and transitions, which had been believed to be unique to human speech (Fitch, 2000b; Fitch and Reby, 2001; Riede et al., 2005). However, the persisting low position of the larynx and hyoid caused by laryngeal descent could provide the basis for less effortful, sophisticated, and rapid rearrangement of the laryngeal position and tongue gesture even in a short single exhalation (Fitch, 2000b). Unfortunately, there is not much information on hyoid movements and on anatomical restrictions to them during vocalization in nonhuman primates. Future studies are needed to examine the presence or absence of this descent in the lineages of platyrrhines and prosimians, or other mammals, and to evaluate the selective advantages of this descent by evaluating variations in the activities of the hyoid, jaw, and tongue in feeding or vocal behaviors.

This study indicates that the growth of the SVT_V is involved in the differences in age-related changes in the proportions of the SVT in early infancy between Japanese macaques and the other two species, whereas the growth of the SVT_H is principally involved in the differences after late infancy between humans and the other two species. It supports the hypothesis (Nishimura et al., 2006) that the reduced growth of the facial length after late infancy—reductions in facial projection and prognathism—established the human SVT configuration and this evolutionary event in the human lineage entailed the evolution of the great descent of the larynx before the divergence of human and chimpanzee lineages. The descent of the laryngeal skeleton relative to the hyoid probably arose in the hominoid lineage after the divergence from the cercopithecoid lineage, whereas the descent of the hyoid preceded this. Thus, the evolutionary path for the great descent of the larynx is likely to be explained by a model of multiple and mosaic evolution, in which the developmental processes involved have arisen in some steps in a long mammalian and primate evolution, under different respective selective advantages. They may have contributed secondarily to the faculty of speech in the human lineage, as one contribution to it. Better understanding of the evolutionary story of the laryngeal descent and human SVT will require continuing efforts to accumulate knowledge on variations in anatomy and physiology of the oral and neck apparatuses in primates.

ACKNOWLEDGMENTS

The authors are grateful to K. Shimizu, M. Ito, T. Kunieda, T. Miyabe, A. Watanabe-Kato, A. Kaneko, S. Hayakawa, S. Araya, W. Yano, M. Tomonaga, and the staff of the Primate Research Institute of Kyoto University for daily veterinary care for the six Japanese macaques and the mothers and/or for support for the MRI examinations. The authors also thank D. E. Lieberman and his colleagues for kindly permitting us to use the numerical data from Lieberman et al. (2001).

APPENDIX

TABLE A1. Spatial resolutions of images acquired and measurements of dimensions

Subjects (sex)	Age (months)	FOV (mm)	Pixel sizes (mm/pixel)	SVT_H (cm)	SVT_V (cm)	HB-PP (cm)	HP-VF (cm)	op* (cm)	lp (cm)
1963 (female)	26	150	0.59	6.14	3.32	3.61	0.41	0.13	1.29
	27	150	0.59	6.16	3.28	3.61	0.39	0.17	1.30
	28	150	0.59	6.31	3.36	3.65	0.36	0.17	1.35
	29	150	0.59	6.34	3.36	3.61	0.40	0.13	1.39
	30	150	0.59	6.36	3.36	3.65	0.39	0.17	1.40
	31	150	0.59	6.44	3.34	3.60	0.42	0.16	1.47
	32	150	0.59	6.45	3.36	3.65	0.44	0.13	1.42
	33	150	0.59	6.53	3.36	3.73	0.40	0.16	1.44
	34	150	0.59	6.85	3.52	3.77	0.44	0.16	1.44
	36	150	0.59	6.87	3.52	3.74	0.44	0.20	1.52
	37	150	0.59	6.93	3.53	3.73	0.44	0.17	1.50
1981 (male)	18	150	0.59	5.90	3.15	3.32	0.58	0.25	1.27
	19	150	0.59	6.03	3.19	3.44	0.60	0.21	1.32
	20	150	0.59	6.16	3.27	3.48	0.60	0.25	1.32
	21	150	0.59	6.10	3.25	3.45	0.54	0.21	1.38
	22	150	0.59	6.22	3.24	3.57	0.57	0.25	1.37
	23	150	0.59	6.29	3.28	3.61	0.55	0.29	1.34
	24	150	0.59	6.29	3.28	3.65	0.59	0.25	1.34
	25	150	0.59	6.35	3.32	3.65	0.62	0.29	1.40
	26	150	0.59	6.62	3.49	3.65	0.62	0.25	1.41
	27	150	0.59	6.64	3.48	3.65	0.66	0.25	1.40
	28	150	0.59	6.75	3.45	3.73	0.64	0.21	1.43
	29	150	0.59	6.85	3.52	3.81	0.64	0.21	1.44
	31	150	0.59	6.95	3.53	3.83	0.68	0.29	1.50
	32	150	0.59	7.04	3.56	3.89	0.71	0.29	1.52
	33	150	0.59	7.14	3.65	3.94	0.79	0.33	1.44
	34	150	0.59	7.25	3.69	3.86	0.77	0.33	1.47
	35	150	0.59	7.27	3.65	3.90	0.71	0.33	1.50
	36	150	0.59	7.29	3.65	3.85	0.79	0.25	1.44

(continued)

TABLE A1. (Continued)

Subjects (sex)	Age (months)	FOV (mm)	Pixel sizes (mm/pixel)	SVT_H (cm)	SVT_V (cm)	HB-PP (cm)	HP-VF (cm)	op[a] (cm)	lp (cm)
2046 (male)	2	120	0.47	3.92	2.04	2.00	0.32	0.03	0.86
	3	120	0.47	4.12	2.13	2.06	0.39	0.03	0.89
	4	120	0.47	4.12	2.15	2.08	0.37	−0.01	0.88
	6	120	0.47	4.42	2.29	2.36	0.33	0.03	0.93
	7	120	0.47	4.54	2.36	2.42	0.39	0.00	1.03
	9	120	0.47	4.91	2.59	2.65	0.41	0.03	1.02
	10	120	0.47	5.13	2.65	2.72	0.40	0.00	1.09
	11	120	0.47	5.25	2.69	2.82	0.45	0.00	1.06
	12	120	0.47	5.30	2.69	2.82	0.42	0.00	1.12
	13	120	0.47	5.43	2.79	2.92	0.44	0.03	1.08
	14	120	0.47	5.46	2.82	2.92	0.44	0.00	1.13
	15	120	0.47	5.56	2.85	2.92	0.44	0.00	1.18
	16	120	0.47	5.59	2.82	2.92	0.48	0.03	1.15
	17	120	0.47	5.79	2.95	2.98	0.51	0.03	1.16
	18	120	0.47	5.79	2.89	2.95	0.49	0.00	1.12
	19	120	0.47	5.87	2.87	3.04	0.47	0.03	1.16
	20	120	0.47	6.00	2.93	3.12	0.44	0.03	1.13
	21	120	0.47	6.08	2.96	3.16	0.42	0.04	1.21
	22	120	0.47	6.09	2.97	3.20	0.45	0.04	1.23
	23	120	0.47	6.22	3.02	3.32	0.45	0.00	1.25
	24	120	0.47	6.39	3.12	3.42	0.47	0.03	1.24
2049 (male)	6	120	0.47	4.64	2.26	2.23	0.33	0.07	0.95
	8	120	0.47	4.83	2.36	2.39	0.36	0.10	0.95
	9	120	0.47	4.98	2.43	2.46	0.36	0.10	0.95
	10	120	0.47	5.07	2.48	2.48	0.36	0.13	1.01
	11	120	0.47	5.22	2.57	2.50	0.37	0.09	1.07
	12	120	0.47	5.29	2.61	2.64	0.35	0.07	1.04
	13	120	0.47	5.28	2.56	2.65	0.39	0.07	1.09
	14	120	0.47	5.33	2.63	2.66	0.40	0.10	1.05
	15	120	0.47	5.48	2.67	2.77	0.31	0.09	1.04
	16	120	0.47	5.55	2.71	2.80	0.32	0.07	1.08
	17	120	0.47	5.65	2.71	2.78	0.34	0.07	1.10
	18	120	0.47	5.69	2.71	2.81	0.30	0.09	1.06
	19	120	0.47	5.78	2.73	2.86	0.38	0.13	1.10
	20	120	0.47	5.86	2.77	2.85	0.34	0.10	1.10
	21	120	0.47	5.93	2.80	2.90	0.41	0.07	1.18
	22	120	0.47	6.04	2.86	2.99	0.42	0.07	1.21
	23	120	0.47	6.15	2.93	3.03	0.38	0.07	1.20
	24	120	0.47	6.22	2.97	3.16	0.36	0.07	1.26
2068 (female)	1	120	0.47	3.90	2.12	2.16	0.16	0.21	0.75
	2	120	0.47	4.10	2.23	2.12	0.18	0.19	0.73
	3	120	0.47	4.13	2.26	2.17	0.23	0.21	0.81
	4	120	0.47	4.24	2.31	2.29	0.25	0.25	0.87
	5	120	0.47	4.34	2.35	2.23	0.27	0.23	0.85
	6	120	0.47	4.51	2.47	2.47	0.23	0.27	0.90
	7	120	0.47	4.56	2.48	2.48	0.29	0.27	0.90
	8	120	0.47	4.89	2.63	2.64	0.30	0.23	1.02
	9	120	0.47	4.94	2.67	2.69	0.28	0.23	1.06
	11	120	0.47	5.13	2.68	2.69	0.35	0.20	1.09
	12	120	0.47	5.35	2.77	2.76	0.33	0.21	1.07
	13	120	0.47	5.40	2.78	2.76	0.38	0.14	1.14
2089 (male)	1	120	0.47	3.92	2.22	2.15	0.31	0.17	0.74
	2	120	0.47	4.01	2.27	2.18	0.33	0.11	0.77
	3	120	0.47	4.25	2.38	2.21	0.47	0.13	0.80
	4	120	0.47	4.27	2.42	2.19	0.47	0.10	0.89
	5	120	0.47	4.37	2.50	2.38	0.40	0.17	0.93
	6	120	0.47	4.47	2.56	2.52	0.37	0.17	1.00
	7	120	0.47	4.62	2.61	2.57	0.39	0.15	0.97
	8	120	0.47	4.81	2.69	2.68	0.37	0.17	1.06
	9	120	0.47	4.89	2.68	2.70	0.42	0.13	1.06
	10	120	0.47	5.01	2.70	2.70	0.40	0.13	1.16
	11	120	0.47	5.06	2.72	2.67	0.46	0.09	1.12
	12	120	0.47	5.24	2.80	2.83	0.46	0.06	1.08

See Subjects and Methods for abbreviations of the dimensions.
[a] Negative values indicate that the epiglottis makes a contact with the velum.

LITERATURE CITED

Ankel-Simons F. 2000. Primate anatomy, 2nd ed. San Diego: Academic Press.

Conroy GC, Mahoney CJ. 1991. Mixed longitudinal study of dental emergency in the chimpanzee. *Pan troglodytes* (Primates, Pongidae). Am J Phys Anthropol 86:243–254.

Crelin ES. 1987. The human vocal tract. New York: Vantage Press.

Crompton AW, German RZ, Thexton AJ. 1997. Mechanism of swallowing and airway protection in infant mammals (*Sus domesticus* and *Macaca fascicularis*). J Zool 241:89–102.

Ekberg O. 1982. Closure of the laryngeal vestibule during deglutition. Acta Otolaryngol 93:123–129.

Ekberg O, Sigurjónsson SV. 1982. Movement of the epiglottis during deglutition. A cineradiographic study. Gastrointest Radiol 7:101–107.

Fant G. 1960. Acoustic theory of speech production. The Hague: Mouton.

Fitch WT. 2000a. The evolution of speech: a comparative review. Trends Cogn Sci 4:258–267.

Fitch WT. 2000b. The phonetic potential of nonhuman vocal tracts: comparative cineradiographic observations of vocalizing animals. Phonetica 57:205–218.

Fitch WT, Giedd J. 1999. Morphology and development of the human vocal tract: a study using magnetic resonance imaging. J Acoust Soc Am 106:1511–1522.

Fitch WT, Reby D. 2001. The descended larynx is not uniquely human. Proc Biol Sci 268:1669–1675.

Flügel C, Rohen JW. 1991. The craniofacial proportions and laryngeal position in monkeys and man of different ages. (A morphometric study based on CT-scans and radiographs). Mech Aging Dev 61:65–83.

Hayama S. 1970. The *Saccus laryngis* in primates. J Anthropol Soc Nippon 78:274-298 (in Japanese with English abstract).

Hewitt G, MacLarnon A, Jones KE. 2002. The functions of laryngeal air sac in primates: a new hypothesis. Folia Primatol 73:70–94.

Hiiemae KM. 2000. The oro-facial complex in macaques: tongue and jaw movements in feeding. In: Whitehead PF, Jolly CJ, editors. Old world monkeym. Cambridge: Cambridge University Press.

Hiiemae KM, Hayenga SM, Reese A. 1995. Patterns of tongue and jaw movement in a cineradiographic study of feeding in the macaque. Arch Oral Biol 3:229–246.

Hiiemae KM, Palmer JB. 1999. Food transport and bolus formation during complete feeding sequences on foods of different initial consistency. Dysphagia 14:31–42.

Hiiemae KM, Palmer JB. 2003. Tongue movements in feeding and speech. Crit Rev Oral Biol Med 14:413–429.

Hiiemae KM, Palmer JB, Medicis SW, Hegener J, Jackson BS, Lieberman DE. 2002. Hyoid and tongue surface movements in specking and eating. Arch Oral Biol 47:11–27.

Hurme VO. 1949. Ranges of normalcy in the eruption of permanent teeth. J Dent Child 16:11–15.

Iwamoto M, Hamada Y, Watanabe T. 1984. Eruption of deciduous teeth in Japanese macaques (*Macaca fuscata*). J Anthropol Soc Nippon 92:273-279 (in Japanese with English abstract).

Iwamoto M, Watanabe T, and Hamada Y. 1987. Eruption of permanent teeth in Japanese monkeys (*Macaca fuscata*). Primate Res 3:18-28 (in Japanese with English abstract).

Kuykendall KL, Mahoney CJ, Conroy GC. 1992. Probit and survival analysis of tooth emergency ages in a mixed-longitudinal sample of chimpanzees (*Pan troglodytes*). Am J Phys Anthropol 89:379–399.

Laitman JT, Crelin ES, Conlogue GJ. 1977. The function of the epiglottis in monkey and man. Yale J Biol Med 50:43–48.

Laitman JT, Reidenberg JS. 1993. Specialization of the human upper respiratory and upper digestive system as seen through comparative and developmental anatomy. Dysphasia 8:318–325.

Larson JE, Herring SW. 1996. Movement of the epiglottis in mammals. Am J Phys Anthropol 100:71–82.

Lieberman DE, McCarthy RC. 1999. The ontogeny of cranial base angulation in humans and chimpanzees and its implications for reconstructing pharyngeal dimensions. J Hum Evol 36:487–517.

Lieberman DE, McCarthy RC, Hiiemae KM, Palmer JB. 2001. Ontogeny of postnatal hyoid and larynx descent in humans. Arch Oral Biol 46:117–128.

Lieberman P. 1984. The biology and evolution of language. Cambridge, MA: Harvard University Press.

Lieberman P, Blumstein SE. 1988. Speech physiology, speech perception, and acoustic phonetics. Cambridge, MA: Harvard University Press.

Lieberman PH, Klatt DH, Wilson WH. 1969. Vocal tract limitations on the vowel repertoires of rhesus monkey and other nonhuman primates. Science 164:1185–1187.

Lysell L, Magnusson B, Thilander B. 1962. Time and order of eruption of the primary teeth: a longitudinal study. Odont Revy 13:217–234.

Negus V. 1949. The comparative anatomy and physiology of the larynx. London: William Heinemann Medical Books.

Nishimura T. 2003. Comparative morphology of the hyo-laryngeal complex in anthropoids: two steps in the evolution of the descent of the larynx. Primates 44:41–49.

Nishimura T. 2005. Developmental changes in the shape of the supralaryngeal vocal tract in chimpanzees. Am J Phys Anthropol 126:193–204.

Nishimura T. 2006. Descent of the larynx in chimpanzees: mosaic and multiple-step evolution of the foundations for human speech. In: Matsuzawa T, Tomonaga M, Tanaka M, editors. Cognitive development in chimpanzees. Tokyo: Springer-Verlag. p 75-95.

Nishimura T, Mikami A, Suzuki J, Matsuzawa T. 2003. Descent of the larynx in chimpanzee infants. Proc Nat Acad Sci USA 100:6930–6933.

Nishimura T, Mikami A, Suzuki J, Matsuzawa T. 2006. Descent of the hyoid in chimpanzees: evolution of face flattening and speech. J Hum Evol 51:244–254.

Nishimura T, Mikami A, Suzuki J, Matsuzawa T. 2007. Development of the laryngeal air sac in chimpanzees. Int J Primatol 28:483–492.

Primate Research Institute, Kyoto University. 2002. Guide for the care and use of laboratory primates, 2nd ed. Inuyama: Primate Research Institute, Kyoto University.

Reidenbach MM. 1997. Anatomical considerations of closure of the laryngeal vestibule during swallowing. Eur Arch Otorhinolaryngol 254:410–412.

Riede T, Bronson E, Hatzikirou H, Zuberbühler K. 2005. Vocal production mechanisms in a non-human primate: morphological data and a model. J Hum Evol 48:85–96.

Roche AF, Barkla DH. 1965. The level of the larynx during childhood. Ann Otol Rhinol Laryngol 74:645–654.

Sasaki CT, Levine PA, Laitman JT, Crelin ES. 1977. Postnatal descent of the epiglottis in man: a preliminary report. Arch Otolaryngol 103:169–171.

Smith BH. 1991. Standard of human tooth formation and dental age assessment. In: Kelley MA, Larsen CS, editors. Advances in dental anthropology. New York: Wiley-Liss. p 143-168.

Smith BH, Garn SM. 1987. Polymorphisms in eruption sequence of permanent teeth in American children. Am J Phys Anthropol 74:289–303.

Starck D, Schneider R. 1960. Respirationsorgane: A. Larynx. In: Hofer H, Schultz AH, Starck D, editors. Primatologia, Vol. 3-2. Basel: Karger. p 423–587.

Stevens KN. 1998. Acoustic phonetics. Cambridge, MA: MIT Press.

Swindler DR, Wood CD. 1973. An atlas of primate gross anatomy. Baboon, chimpanzees, and man. Seattle: University of Washington Press.

Takemoto H. 2001. Morphological analyses of the human tongue musculature for three-dimensional modeling. J Speech Lang Hearing Res 44:95–107.

Titze IR. 1994. Principles of voice production. Englewood Cliffs: Prentice-Hall.

Vandaele DJ, Perlman AL, Cassell MD. 1995. Intrinsic fibre architecture and attachments of the human epiglottis and their contributions to the mechanism of deglutition. J Anat 186:1–15.

Vorporian HK, Kent RD, Gentry LR, Yandell BS. 1999. Magnetic resonance imaging procedures to study the concurrent anatomic development of vocal tract structures: preliminary results. Int J Pediat Otorhinolaryngol 49:197–206.

Williams PL, editor. 1995. Gray's anatomy. 38th ed. New York: Churchill Livingstone.

Westhorpe RN. 1987. The position of the larynx in children and its relationship to ease of intubation. Anaesth Intens Care 15: 384–388.

Zemlin WR. 1988. Speech and hearing science: anatomy and physiology. 3rd ed. Englewood Cliffs: Prentice-Hall.

Available online at www.sciencedirect.com

ScienceDirect

Journal of Nutritional Biochemistry 19 (2008) 524–535

Journal of Nutritional Biochemistry

Allicin inhibits cell growth and induces apoptosis through the mitochondrial pathway in HL60 and U937 cells

Talia Miron[a,*], Meir Wilchek[a], Ayala Sharp[b], Yoshihito Nakagawa[c], Makoto Naoi[c], Yoshinori Nozawa[c], Yukihiro Akao[c]

[a]*Department of Biological Chemistry, Weizmann Institute of Science, Rehovot 76100, Israel*
[b]*Department of Biological Services, Weizmann Institute of Science, Rehovot 76100, Israel*
[c]*Gifu International Institute of Biotechnology, Kakamigahara, Gifu 504-0838, Japan*

Received 22 April 2007; received in revised form 12 June 2007; accepted 20 June 2007

Abstract

In this article, the effects of allicin, a biological active compound of garlic, on HL60 and U937 cell lines were examined. Allicin induced growth inhibition and elicited apoptotic events such as blebbing, mitochondrial membrane depolarization, cytochrome *c* release into the cytosol, activation of caspase 9 and caspase 3 and DNA fragmentation. Pretreatment of HL60 cells with cyclosporine A, an inhibitor of the mitochondrial permeability transition pore (mPTP), inhibited allicin-treated cell death. HL60 cell survival after 1 h pretreatment with cyclosporine A, followed by 16 h in presence of allicin (5 μM) was ~80% compared to allicin treatment alone (~50%). Also *N*-acetyl cysteine, a reduced glutathione (GSH) precursor, prevented cell death. The effects of cyclosporine A and *N*-acetyl cysteine suggest the involvement of mPTP and intracellular GSH level in the cytotoxicity. Indeed, allicin depleted GSH in the cytosol and mitochondria, and buthionine sulfoximine, a specific inhibitor of GSH synthesis, significantly augmented allicin-induced apoptosis. In HL60 cells treated with allicin (5 μM, 30 min) the redox state for 2GSH/oxidized glutathione shifted from E_{GSH} −240 to −170 mV. The same shift was observed in U937 cells treated with allicin at a higher concentration for a longer period of incubation (20 μM, 2 h). The apoptotic events induced by various concentrations of allicin correlate to intracellular GSH levels in the two cell types tested (HL60: 3.7 nmol/10^6 cells; U937: 7.7 nmol/10^6 cells). The emerging mechanistic basis for the antiproliferative function of allicin, therefore, involves the activation of the mitochondrial apoptotic pathway by GSH depletion and by changes in the intracellular redox status.

Keywords: Allicin; Apoptosis; Garlic; GSH; HL60; U937

1. Introduction

Allicin, diallyl thiosulfinate, is the main biologically active compound derived from garlic. It is produced by the interaction of the enzyme alliinase (alliin lyase; EC 4.4.1.4) with its substrate alliin (*S*-allyl-L-cysteine sulfoxide) [1]. Since alliinase and alliin are enclosed in different compartments within the garlic clove cells, intact garlic cloves do not contain allicin. When the garlic clove is crushed, alliin and alliinase interact, to form allicin, pyruvic acid and ammonia (Scheme 1). Allicin became an object of interest due to its potential to confer a vast spectrum of health beneficial effects including: anti microbial, antifungal and antiparasitic [2], antihypertensive [3], cardioprotective [4–6], anti-inflammatory [7] and anticancer activities [2,8,9].

In vitro studies of allicin's effect on human mammary MCF-7 cancer cells revealed that its antiproliferative activity is accompanied by accumulation of cells in the regulatory checkpoints, G_0/G_1 and G_2/M, of the cell cycle [9]. Interestingly, also other ally sulfur compound cause similar effects [10]. Allicin was shown to induce apoptosis in gastric

Abbreviations: BSO, D,L-buthionine *S,R*-sulfoximine; CsA, Cyclosporin A; DTNB, 5,5′-dithiobis-(2-nitrobenzoic acid); GGCS, γ-Glutamyl-L-cysteine synthetase; GSH, Reduced glutathione; GSSA, *S*-allylmercaptoglutathione; GSSG, Oxidized glutathione; mPTP, Mitochondrial permeability transition pore; NAC, *N*-acetyl-L-cysteine; XTT, 2,3-Bis (2-methoxy-4-nitro-5-sulfophenyl)-2*H*-tetrazolium-5-carboxanilide sodium salt.

* Corresponding author. Tel.: +972 8 9343627; fax: +972 8 9468256.
E-mail address: talia.miron@weizmann.ac.il (T. Miron).

0955-2863/$ – see front matter © 2008 Elsevier Inc. All rights reserved.
doi:10.1016/j.jnutbio.2007.06.009

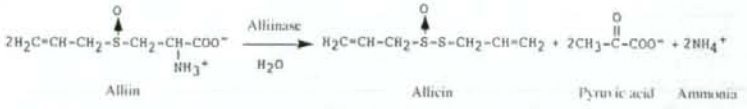

Scheme 1.

cancer SGC-7901 cells. The cause of apoptosis was related to decreased telomerase activity, an enzyme which allicin inhibits in a time- and dose- dependent manner [11]. Allicin induces apoptosis in human cervical cancer SiHa cells and mouse fibroblast-like L-929 cells, manifested through the appearance of characteristic apoptotic morphological changes in apoptotic bodies, through DNA fragmentation, and activation of caspases 8, 9 and 3 [12]. Allicin was also shown to induce apoptosis in human epithelial carcinoma through a caspase-independent pathway, mediated by the release of apoptotic-inducing factor (AIF) from mitochondria and protein kinase A (PKA) activation [13]. More results describing the effects of allicin or other garlic-derived products on various proteins participate in the apoptotic process have already been reported [14]. However, the mechanism underlying the induction of cell death by allicin has not been fully elucidated.

Apoptosis is an ordered cascade of events that culminates in cell death. Two main pathways of apoptosis have been characterized. The extrinsic pathway is initiated through ligand stimulation of the cell surface death receptors such as TNFR or CD95R. In this pathway, cell death is executed via a cascade of proteolytic events with the sequential activation of caspase 8 and caspase 3. The intrinsic pathway is triggered by mitochondrial stress caused by various factors such as DNA damage, oxidative stress and heat shock (reviewed [15]). This pathway is initiated through the release of signal factors from mitochondria as a consequence of mitochondrial membrane permeability transition. Such changes lead to translocation of pro- and antiapoptotic proteins across the mitochondrial membranes [16,17]. Among these proteins is cytochrome *c*, which is released from the mitochondria to the cytosol and participates with other molecules in the formation of a complex that activates caspase 9, which in turn activates caspase 3. The activation of these caspases leads to the final fragmentation of nuclear DNA, with the typical apoptotic morphological manifestations.

Allicin easily diffuses through cell membranes (diffusion coefficient 5×10^{-8} cm^2s^{-1}) [18] and exerts its biological effects by reacting with free thiols within the cell. In living cells, reduced glutathione (GSH) is the major free thiol participating in cellular redox reactions and mixed disulfide formation. GSH is therefore the main cellular target of allicin reaction (Scheme 2). Both allicin and its glutathione derivative, *S*-allylmercaptoglutathione (GSSA), can prevent the formation of free radicals. GSSA is similar in this preventive capacity to GSH, both being less effective in this antioxidant activity than allicin [19–21]. Allicin can scavenge the chain-carrying peroxyl radicals of the substrates by transferring its allylic hydrogen to the oxidized substrate. This renders it a stronger antioxidant than its derivatives [22].

Allicin is a short-lived compound, which rapidly reacts with free intracellular thiol groups [18,19,22]. It was found to disintegrate in the blood a few minutes after its administration, both in vitro in human blood [23] and in vivo in rats [24]. Therefore, the therapeutic effect of allicin administered orally may be restricted to targets that are close to the gastrointestinal tract. However, its main oxidation products, *S*-allylmercapto-glutathione and *S*-allylmercapto-cysteine, could exert their action in more remote sites within the body because they are more stable. The rapid disappearance of allicin can be exploited in tumor cells targeting. We previously showed that allicin kills tumor cells in vitro [25,26] and also in vivo if generated on their surface by conjugating alliinase to monoclonal antibodies directed to specific cell-surface receptors, such as ErbB2, overexpressed in breast and ovarian cancer [25]; CD20, a receptor expressed at high levels in human B chronic lymphocytic leukemia and other B-cell lymphomas [26].

The redox environment of a cell reflects the sum of the products of the reduction potential and the reducing capacity of the linked redox couples operating within the cell [27,28] Glutathione is considered to be the major thiol-disulfide redox buffer of cells [29]. The redox state of the 2GSH/oxidized glutathione (GSSG) redox couple depends on their molar ratio. Upon reacting with GSH, allicin causes a decrease in free GSH concentration and an increase in mixed-disulfide glutathione products, which leads to an increase in the reduction potential values. Allicin also reacts with other

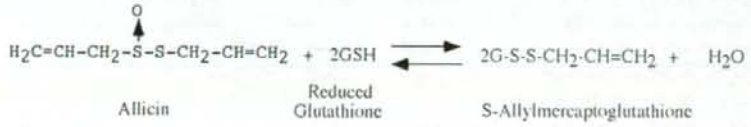

Scheme 2.

free sulfhydril (SH)-bearing molecules in the cell, such as cysteine and SH residues in proteins, yet their relatively low concentrations contribute only little towards changing the reduction potential of the cell upon oxidation. The reduction potential of cells was proposed to reflect their growth cycle. Accordingly, the reduction potential of proliferating cells (pH 7.0) is E_{GSH} −240 mV. Increased values (E_{GSH} −200 mV) represent differentiation, and a further oxidative shift to a higher value (E_{GSH} −170 mV) elicits apoptosis [27]. In this study, we aimed to examine the initial events leading to apoptosis upon allicin treatment and the dependence of the apoptotic pathway on the reduction potential of cells.

2. Materials and methods

Alliin was synthesized from L-cysteine and allyl bromide followed by H_2O_2 oxidation [30]. Allicin (purity ~98%) was produced by applying synthetic alliin onto an immobilized alliinase column and its concentration was determined by high-performance liquid chromatography, as previously described [31].

2,3-Bis (2-methoxy-4-nitro-5-sulfophenyl)-2 *H*-tetrazolium-5-carboxanilide (XTT) sodium salt; D,L-buthionine *S*, *R*-sulfoximine (BSO); cyclosporin A (CsA); *N*-acetyl-L-cysteine (NAC); 5,5′-dithiobis-(2-nitrobenzoic acid) (DTNB); metaphosphoric acid; phenazine methosulfate (PMS) and 2-vinylpyridine were purchased from Sigma Chemical (St. Louis, MO, USA).

2.1. Cell culture, cell viability and morphological studies.

HL60 human promyelocytic leukemia-derived cells and U937 human myelomonocytic cells were maintained in RPMI-1640 supplemented with 2 mM L-glutamine, 10% (v/v) fetal bovine serum and antibiotics. Cell viability was measured using the XTT assay, based on the reduction of tetrazolium salt to soluble formazan compounds by mitochondrial enzymes. Cells (15.000–20.000 cells/well) were seeded in a 96-well plate. After 16-h incubation with allicin, in the presence or absence of NAC (0.1–1.0 mM) or after 16 h incubation with BSO (0.1 mM) alone, 50 μl of XTT/PMS mixture (50 μM PMS, 0.1% XTT in medium) were added onto the cells. After an incubation period of 3–4 h at 37°C, the absorbance of the samples was measured in an enzyme-linked immunosorbent assay (ELISA) reader at 450 nm. SDS (1%, 10 μl/well) was added to reference wells before adding the XTT/PMS solution.

HL60 cells (300,000/ml) were pretreated with CsA for 1 h. Cells were seeded in a 96-well plate (20,000 cells/well) in the presence of allicin. The viability was tested by the XTT assay. The analysis of apoptotic morphological changes was done by staining cells with Hoechst 33342 at 37°C for 30 min in medium, washing with phosphate-buffered saline (PBS) and examining by fluorescence microscopy. For evaluating DNA ladder formation, cellular DNA was extracted from cells by ethanol precipitation of the phenol/chloroform extract [32]. After electrophoresis (5–10 μg DNA/lane) on an agarose (2.5%) gel, DNA was visualized by ethidium bromide staining.

Mitochondrial membrane potential was measured by using the fluorescent dye, Mito Tracker Red CMXRos (Molecular Probes, Eugene, OR, USA) that accumulates selectively in active mitochondria. Cells were washed with medium, incubated with Mito-Tracker Red CMXRos for 30 min at 37°C, washed with PBS and examined under fluorescence microscopy (Olympus, Tokyo).

Mitochondria were prepared from cultured cells (5–10×10^7) as described elsewhere [33]. Cells were harvested and washed with PBS (600 g, 7 min). Cell pellets were suspended in 0.5 ml cold hepes isotonic mitochondrial buffer (HIM) buffer (200 mM mannitol, 70 mM sucrose, 1 mM EGTA, 10 mM HEPES-KOH buffer, pH 7.5) containing protease inhibitors, incubated 30 min on ice and homogenized by multiple passages through a 25-gauge needle (5/8 in.). Nuclei and unbroken cells were removed (1300 g, 8 min at 4°C). Protein and free SH were determined in the cytosol, supernatant (10,000 g, 30 min at 4°C) and in the mitochondria-enriched fraction (pellet, dissolved in HIM buffer containing 1% Triton X-100). Protein assay was done with the Biuret Reagent [34] or the BCA protein assay kit (Pierce, Rockford, IL, USA).

2.2. Cell cycle analysis

HL60 cells were pretreated with CsA (5 μM, 1 h) and then cultured further for 20 h in the presence or absence of allicin. After harvesting, washing and resuspending in 0.25 ml PBS, an equal volume of 0.005% propidium iodide solution containing 0.01% heated-RNase A and 0.3% Triton X-100 was added. Cells were analyzed by flow cytometry using fluorescence-activated cell sorting (Becton Dickinson FACScan Instrument using CellQuest software (BD Bioscience, San Jose, CA, USA).

2.3. Electrophoresis and Western blot analysis

Cell pellet was resuspended in lysis buffers A or B [32]. Lysis buffer A (2×PBS, 0.1% sodium dodecyl sulfate (SDS), 1% Nonidet P-40, 0.5% sodium deoxycholate) containing protease inhibitors was used to analyze of caspases 3, 8 and 9. Lysis buffer B (250 mM sucrose, 20 mM HEPES-KOH buffer, pH 7.5, 10 mM KCl, 1.5 mM $MgCl_2$, 1 mM EDTA, 1 mM EGTA, 1 mM dithiothreitol [DTT]) containing protease inhibitors was used to analyze the presence of cytochrome *c* in the cytosol as described above (Section 2.2), After centrifugation (10,000g, 30 min, 4°C) the supernatant was separated by SDS-polyacrylamide gel electrophoresis using 15% gel and transferred electrophoretically onto a polyvinylidene difluoride (PVDF) membrane (Du Pont, Boston, MA, USA). The membrane was incubated overnight at 4°C with the following antihuman antibodies: anti β-actin (Sigma–Aldrich), anti-caspase 3 (Santa Cruz Biotechnology, Santa Cruz, CA, USA), anti-caspase 8 (MBL, Nagoya, Japan), anti

caspase-9 (Novus Biological, Littleton, CO, USA) and anti cytochrome *c* (Upstate Biotechnology, Lake Placid, NY, USA). The membranes were washed with tris-buffered saline Tween-20 (TBST), incubated with HRP-conjugated secondary antibody for 1 h at room temperature and washed with TBST. Proteins were detected with an enhanced chemiluminescence (ECL) detection kit (New England Biolabs) and a chemiluminescence detector (LAS-1000, Fuji, Japan).

2.4. Determination of cell volume

The volume of nontreated cells was determined by calculating sphere volumes based on diameter measurement of 100 cells. Since the morphology of treated cells was not spherical, cell volume was estimated by weighing the pellet of $2–4\times10^6$ cells and evaluating the volume on the assumption of 1/1 w/v.

2.5. Assay for glutathione and free SH

Cells were collected (600 g, 7 min, 4°C), washed with PBS and the pellets were stored at −80°C. After protein precipitation with 5% metaphosphoric acid (0.2–0.3 ml/3×10^6 cells) by centrifugation (10,000*g*, for 30 min), the supernatant was used for GSH quantitation, and the pellet, dissolved in 0.2–0.3 ml of 0.5 M NaOH, was used for protein determination. To determine GSH in the supernatant, a glutathione assay kit (Calbiochem) was used. GSH and GSSG content were also determined by the glutathione reductase recycling assay before and after modification with 2-vinyl pyridine [35]. Samples (40 μl) were neutralized with 2 M triethanolamine (10 μl) in a 96-well plate. The reaction was started by adding 200 μl per well of 0.4 U/ml enzyme in 143 mM phosphate buffer pH 7.5 containing 0.3 mM reduced nicotinamide adenine dinucleotide phosphate, 0.6 mM DTNB and 6.25 mM EDTA. The initial rate of 5-thio-2-nitrobenzoic acid formation was monitored. Determination of GSSG was done 1 h after modification of the free SH with 9 M 2-vinyl pyridine (1 μl/well) at room temperature. Oxidized glutathione (0–6 nmol/well) served as a reference.

Total free SH content in cell extracts or in cytosolic and mitochondrial fractions (50 μl) was determined with DTNB in a 96-well plate. Samples were acidified with 5% metaphosphoric acid (50 μl/well) to stabilize the reduced state and neutralized with 2 M triethanolamine (50 μl/well). DTNB (50 μl of 1 mM solution in 50 mM phosphate buffer pH 7.2 containing 2 mM EDTA) was added. After 10 min of incubation, the absorbance was measured at 412 nm using an ELISA reader. GSH (0–20 nmol/well) precalibrated with DTNB served as a reference, using E_M 14150 M^{-1} at 412 nm [36]. Reduction potential was calculated by using the Nernst equation for GSSG/2GSH: $E_{GSH}=E_0-30\times\log([GSH]^2/[GSSG])$ [27].

2.6. Statistical analysis

Each experiment was performed at least three times, and the results were expressed as mean values± S.D. (n=2–6). The Student t test was used to determine the significance of differences between the mean values obtained for the two cell lines. Otherwise, the various treatments, were analyzed using one-way analysis of variance (ANOVA) followed by either Dunnett or Bonferroni's multiple comparison test, considering $P<05$ as significant.

3. Results

3.1. Allicin inhibited proliferation of HL60 and U937 cells

The proliferation rate of exponentially growing HL60 and U937 cells in the presence of allicin was determined at a density of 100,000 cells ml^{-1}. Cells were incubated with increasing concentrations of allicin (HL60: 0–10 μM; U937: 0–30 μM) for growing time periods up to 72 h. Cell viability was determined by the trypan blue dye exclusion assay. Allicin inhibited cell growth in a concentration-dependent manner (Figs. 1A and 2A for HL60 and U937, respectively). In the presence of 5 μM allicin, HL60 cells exhibited about 50% inhibition of proliferation after 22 h, and at 10 μM allicin after 22 h, the rate of inhibition reached 80% (Fig. 1A). HL60 cells were more sensitive to allicin than U937 cells. Inhibition of U937 cell proliferation reached 50% and 60% at 15 and 20 μM allicin, respectively, after 22 h (Fig. 2A). We therefore chose to continue the study of HL60 and U937 cells (100,000 cells/ml) at 5 and 20 μM allicin, respectively.

3.2. Allicin induced apoptosis in the cells

3.2.1. Morphological changes

Morphological changes indicating apoptotic processes were observed by staining the cells with Hoechst 33342. Distinct nuclear condensation was observed in HL60 cells treated with allicin (5 μM) for 16 h (Fig. 1B) and U937 cells treated with allicin (20 μM) for 40 h (Fig. 2B). In both allicin-treated cell lines, more than 90% of the cells showed blebbing after 2 h (Fig. 3A, lower panel).

3.2.2. DNA fragmentation

A DNA ladder appeared in allicin (5 μM)-treated HL60 cells 6 h after treatment, whereas in allicin (20 μM)-treated U937 cells, it appeared only after 40 h (Figs. 1C and 2C).

3.2.3. Cytochrome c release into cytoplasm and activation of caspases

To better understand the mechanism of allicin-induced apoptosis, Western blot analysis was used to detect apoptosis-related proteins. Increased amounts of cytochrome *c* appeared in the cytosol of allicin (5 μM)-treated HL60 cells after 2.5 h of incubation. An increase in cleaved caspase 9 appeared 4 and 6 h after adding allicin, and it gradually decreased to the basal level after 30 h. Cleaved caspase 3 appeared after 16 h and was still observed 30 h after the treatment (Fig. 3B). U937 cells reacted at a slower rate to allicin (20 μM) treatment. Cytochrome *c* release into the cytosol began 6 h after adding allicin and reached a maximal

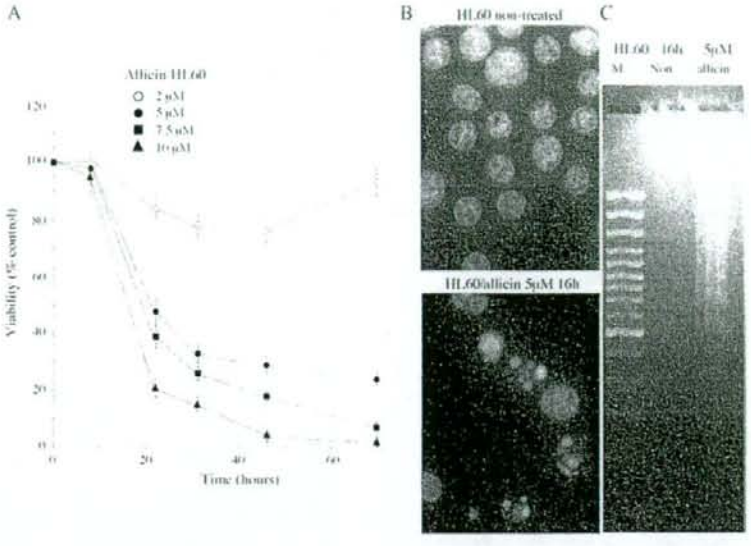

Fig. 1. Effect of allicin on cell growth of human leukemia HL60 cells. (A) Growth dependent of HL60 cells on allicin concentration. Viable cells were counted at various time intervals between 0–72 h after staining with trypan blue. Data represent the mean value of % viable cells (nontreated=100%)±S.D. (B) Apoptotic changes observed after Hoechst 33342 (5 μg/ml) staining for 30 min. Cells were treated with 5 μM allicin for 16 h. (C) Nucleosomal DNA fragmentation of nontreated cells and allicin-treated HL60 cells (5 μM, 6 h, 5 μg/lane). Lane M is a DNA size marker.

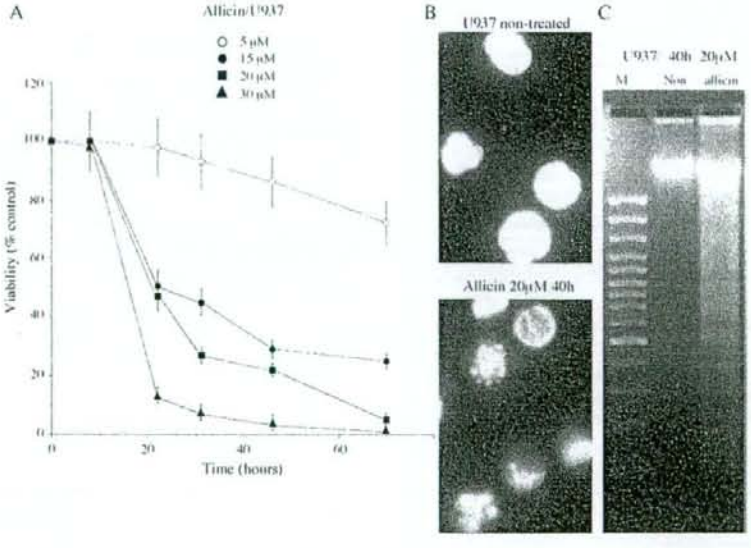

Fig. 2. Effect of allicin on cell growth of human leukemia U937 cells. (A) Growth dependence of U937 cells on allicin concentration. Viable cells were counted at various time intervals between 0–72 h after staining with trypan blue. Data represent the mean value of % viable cells (nontreated=100%)±S.D. (B) Hoechst 33342 (5 μg/ml) staining for 30 min of cells treated with 20 μM allicin for 40 h. (C) Nucleosomal DNA fragmentation of nontreated cells and allicin-treated U937 cells (20 μM, 40 h, 10 μg/lane). Lane M is a DNA size marker.